Planar and High-Resolution SPECT Bone Imaging in the Diagnosis of Facet Syndrome

Lawrence E. Holder, Jane L. Machin, Paul L. Asdourian, Jonathan M. Links and Carlton C. Sexton

Division of Nuclear Medicine, Department of Diagnostic Radiology, The University of Maryland Medical System; Departments of Nuclear Medicine, Orthopedics and Radiology, The Union Memorial Hospital; Division of Nuclear Medicine, Department of Radiology, The Johns Hopkins Medical Institutions, Baltimore, Maryland

This study's goals were to determine the appearance of potentially symptomatic facet joints on planar and high-resolution SPECT radionuclide bone imaging, relate the relative sensitivity of the two techniques and assess the predictive value in a clinical setting. **Methods:** Fifty-eight consecutive patients referred with a diagnosis of possible facet syndrome were imaged during the same visit using both a well-established planar and a SPECT technique developed to emphasize high spatial resolution. The standard of reference included facet injections with a marcaine and steroid mixture, with review of a pain journal completed by the patient included in the followup criteria. **Results:** In the 43 patients comprising the final study group, 7 were diagnosed with facet syndrome, 5 with abnormal planar images and 7 with abnormal SPECT images. A total of 10 facet joints with abnormal increased uptake were seen on SPECT which were not demonstrated on planar imaging. There was high sensitivity (100% SPECT, 71% planar), but somewhat lower specificity (71% SPECT, 76% planar). The negative predictive value was high (100% SPECT, 93% planar). Radionuclide bone imaging additionally discovered a nonfacet joint etiology for patient symptoms in 16 of the 43 patients. **Conclusion:** Higher spatial resolution SPECT images are better accepted by referring physicians who correlate them with CT or MR images. The high negative predictive value allows radionuclide bone imaging to be used to select appropriate patients to undergo the invasive facet injection procedure.

Key Words: bone imaging; SPECT, bone; facet syndrome; back pain; radionuclide imaging, bone

J Nucl Med 1995; 36:37–44

FIGURE 1. Transaxial wet specimen at L4-5. Facet joints are true synovial joints with hyaline cartilage (long arrow) lined with synovial membrane and surrounded by a fibrous capsule (short arrow). Each joint is supplied by branches from at least two posterior rami. Parts of the cauda equina are seen in the spinal canal (arrowhead). The inferior facet of L4 (4) is posterior to the superior facet of L5 (5).

Facet syndrome, or posterior spinal compartment syndrome, the existence of which remains controversial (*1*), is an articular disorder related to the lumbar facet joints and their innervations (*2*) (Fig. 1). It produces both local and radiating pain, which is often ill-defined with absent specific neurological findings (*3*). Ghormley first coined the term facet syndrome in discussing alternative sources of low back pain with leg radiation (*4*). In 1975, Mooney and Robertson reviewed the anatomy of the joint and its nerve supply in some detail as it related to the clinical syndrome and to their attempts at therapy (*5*) (Fig. 2).

Procedures have been developed to either denervate or obliterate the facets under the assumption that these articulations are a significant source of pain. Unilateral or bilateral procedures have been performed indiscriminately to the lowest two lumbar segments, which are the earliest to degenerate in most patients. More recently, Berquist has reviewed the topic in relation to modern diagnostic and therapeutic injection therapy (*6*). Differentiation between disk disease and facet syndrome can be difficult clinically, and in general most patients have been evaluated for disk

Received Jan. 27, 1994; revision accepted Jul. 21, 1994.

For correspondence and reprints contact: Lawrence E. Holder, MD, Division of Nuclear Medicine, Department of Radiology, University of Maryland Medical Center, 22 South Greene St., Baltimore, MD 21201-1595.

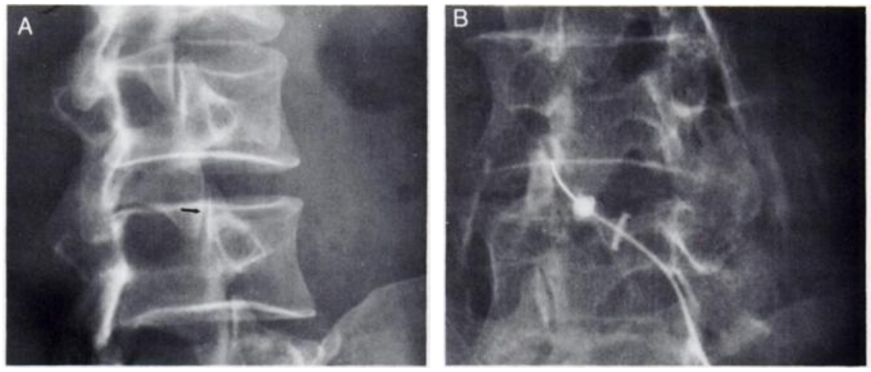

FIGURE 2. X-ray of facet joint. (A) Normal. The facet joints become more oblique and laterally oriented as one progresses from L1 through L5. The normal facet joint, viewed tangentially, is 2–3 mm wide with sharp margins and a well demarcated cortex (arrow). (B) Abnormal. The earliest changes in arthritis appeared to be sclerosis followed by progressive narrowing of the joint and bony eburnation at the margins of the joint. Needle is seen during injection with tip localized to facet joint under fluoroscopy.

disease with CT (Fig. 3) or MRI (Fig. 4) before facet syndrome has been considered. There is no reported correlation of symptoms with plain radiographic or CT evidence of degeneration of the facet joints.

Other authors have related planar imaging, SPECT imaging and CT scanning in the lumbar spine (*7–9*). Many different techniques were used, and the clinical significance of results were left for later study. These reports suggested that in some cases, localization of tracer activity could be improved with SPECT, and that often additional foci of abnormal tracer uptake could be identified. Because of our specific interest in facet syndrome, we evaluated 58 patients referred for facet syndrome to determine the appearance of potentially symptomatic facet joints on planar and SPECT radionuclide bone images. We wanted to relate the sensitivity of planar imaging findings to those of a high-resolution SPECT technique, and to assess the predictive value of radionuclide bone imaging in a clinical setting.

MATERIALS AND METHODS

Patient Population

From July 1991 to December 1992, there were 58 patients referred with a diagnosis of possible facet syndrome. They included 24 males and 34 females, aged 14–82 yr, with a mean age of 53 yr. Nine patients with prior surgery, known spondylolysis or concurrent intervertebral disk herniation were excluded. Six patients were lost to follow-up, so the final study

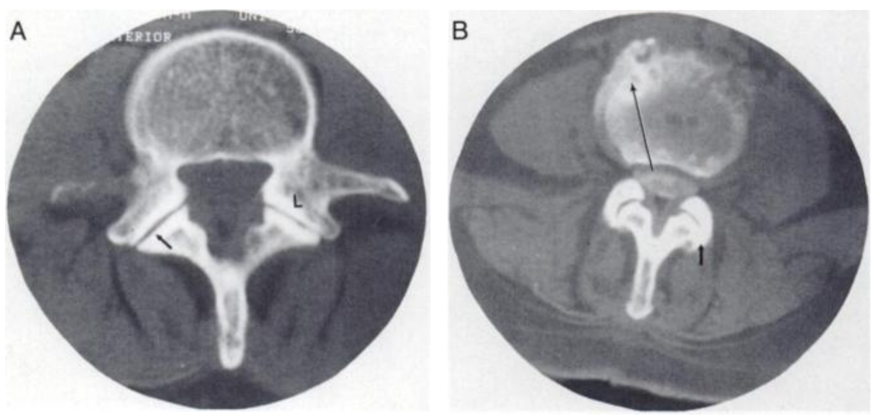

FIGURE 3. CT scans. (A) Normal. Berquist has emphasized the progressive lateral oblique positioning of the lumbar facet joints. At this L4-5 level on right, the joint is normal in width with sharp cortical margins (arrow). On the left, there is early joint narrowing and sclerosis. (B) Abnormal. Joint narrowing, sclerosis and hypertrophic spur formation (short arrow) can often be better defined on CT than on plain radiographs. This image also demonstrates anterior degenerative change of the vertebral body (long arrow).

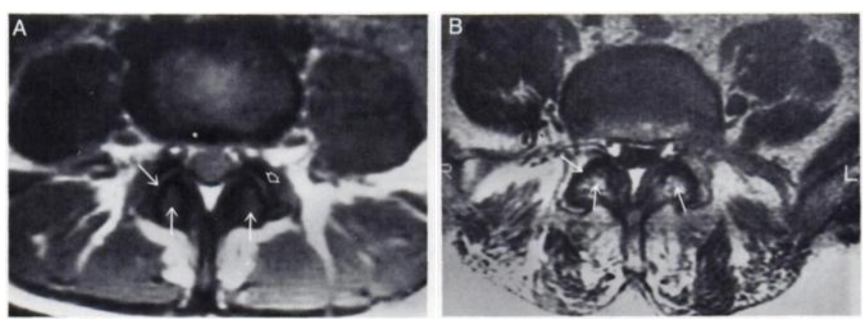

FIGURE 4. MR Image. (A) Normal. Axial proton density image through inferior aspect of L4-5. Joint has normal space with brighter signal representing combined synovial sack and adjacent cartilage (open arrow). The well defined cortical edge with its low-intensity black signal (straight arrow) and normal brighter marrow signal intensity in inferior facet of L4 (arrowheads) are well seen. (B) Abnormal, facet arthritis. Axial T1-weighted image through the inferior aspect of L4-5 disc space. Bilateral large facet osteophytes are present. Sclerotic and thickened cortical bone has a black signal (arrow) and marrow has brighter signal (arrowheads).

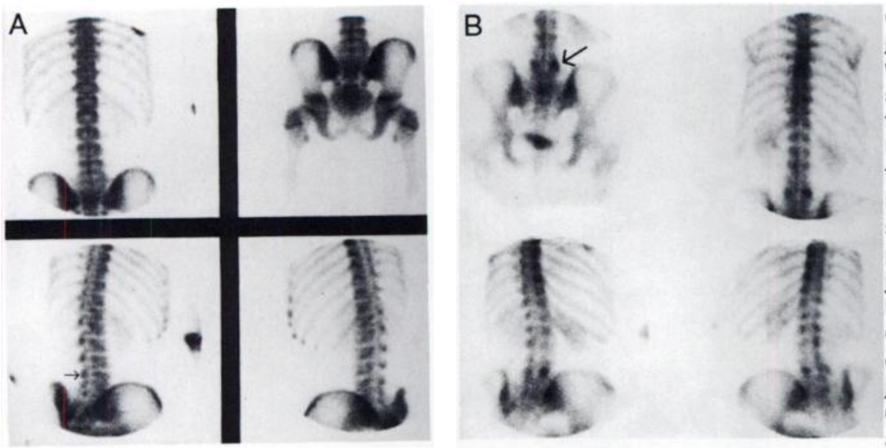

FIGURE 5. Planar delayed radionuclide bone scan. (A) Normal. Compare these images to normal x-ray (Fig. 2A). In addition to sharp endplates, spinous processes, and transverse processes, the oblique views demonstrate the position of the facet joints just anterior to the region of the spinal canal which is relatively more photon deficient and seen anterior to the projection of the contralateral posterior elements (straight arrow). Because referred pain is common, note that the large field of view camera allows us to image significant portions of the thoracic spine. We also routinely obtain views of the pelvis and hips. (B) Abnormal. Bilateral facet joint uptake right (arrow) more marked than left. Note the orientation of the facet activity on the RPO view (lower left image) and compare with the orientation of the facet joints on Figure 2A and appreciate that this orientation is 90° to the orientation of the adjacent pars region.

group consisted of 43 patients, including 17 males and 26 females, aged 16–82 yr, with a mean of 55 yr. In addition to symptoms suggesting possible facet syndrome, all patients had some anatomic evidence of facet arthritis: plain x-ray (n = 42), CT (n = 11) or MRI (n = 21). Their symptoms had been present for 1 wk to 7 yr, with 16 patients for 6 mo or less and 27 patients for more than 6 mo.

Scintigraphy

Delayed planar imaging was performed using the following parameters: dose: 25 mCi (925 MBq) of ^{99m}Tc MDP (Osteolite) intraveneously; delay: 3 hr with vigorous hydration; Camera: 75 PM tube gamma camera, 1/4″ crystal, acquired 9/87; high-resolution collimator; Images: 1,000K counts per view; Views: Posterior, LPO and RPO lumbar spine, posterior pelvis, anterior lumbar spine (Fig. 5).

SPECT was performed immediately after planar imaging. In order to design an appropriate SPECT acquisition, reconstruction and display protocol specifically tailored to facet imaging, we met with the referring clinicians. We identified high anatomic resolution as the most important criterion in order to best compare SPECT images with those from CT. Accordingly, we designed our SPECT protocol to maximize spatial resolution. In order to do so, we addressed three issues: choice of collimation, sampling and reconstruction filter, all of which will be discussed. Data were acquired using the following parameters: Camera: 61 PM tube gamma camera, 1/2″ crystal, acquired 5/83; high-resolution collimator, long bore holes; 360° elliptical orbit; 128 projections; 15 sec per projection, 128 × 128 matrix. The counts per projection image ranged from 20,000 to 25,500 with total study counts from 2,560,000 to 3,264,000. Processing parameters: Hanning pre filter, 1.4 cycles/cm critical frequency; ramp filtered backprojection; 1 pixel (3.2 mm) thick slices (Figs. 6–9).

In order to maximize spatial resolution and to minimize the change in resolution with distance from the collimator face, we used a high-resolution collimator with long bore holes.

In order to appropriately digitally sample the (high resolution) analog camera signals, we used a 128 × 128 matrix to represent each projection. In order to make the angular sampling at least as equivalent to the linear projection sampling, (i.e., the pixel size in a projection), we used the following approach.

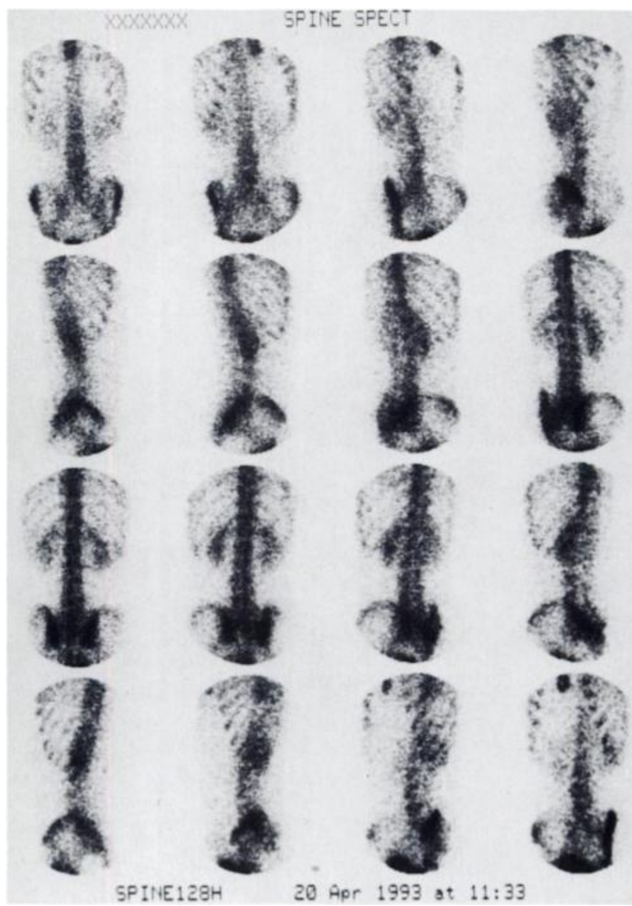

FIGURE 6. Raw projection data. 128 images, 15 sec/image, 360° orbit, ~3° steps. Every eighth image displayed.

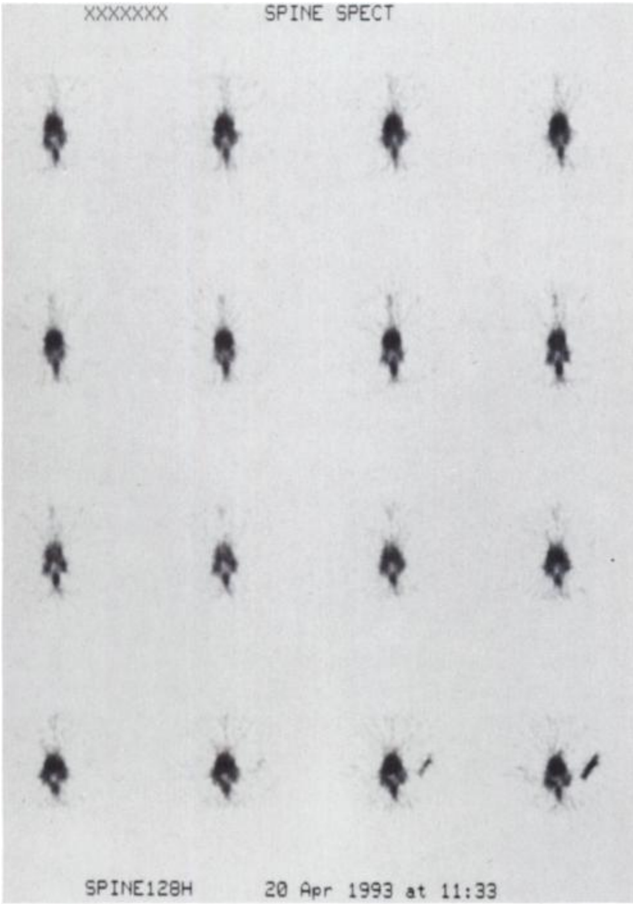

FIGURE 7. Transaxial slice reconstruction with 1-pixel thick slices. Displayed from cranial, upper left to caudal, lower right.

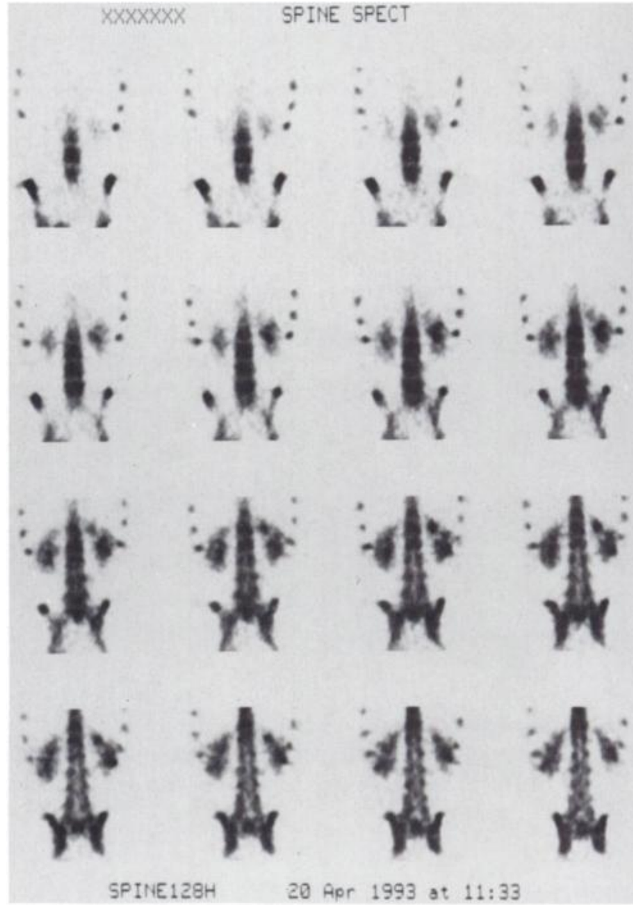

FIGURE 8. Coronal slices reconstructed from transaxial slice data with 1-pixel thick slices. Displayed from anterior upper left to posterior, lower right.

This linear pixel size was given by:

$$\text{linear pixel size} = \frac{\text{body diameter}}{\text{number of pixels spanning body}}.$$

The angular sampling interval was considered to be the angular step interval and was given by:

$$\text{angular step size} = \frac{\pi \times \text{body diameter}}{\text{number of projections}}.$$

Setting these equal, the relationship between linear pixel size and angular step size was given by:

$$\text{linear pixel size} = \text{angular step size}$$

$$= \frac{\text{body diameter}}{\text{number of pixels spanning body}}$$

$$= \frac{\pi \times \text{body diameter}}{\text{number of projections}}.$$

Thus, there needed to be π times as many projections around 360° as there were pixels spanning the body. This simplified rule of thumb only applies when the attenuation is such that the anterior 180° of data contain no posterior information and when the posterior 180° of acquisition contains no anterior data. In practice, because of the monoexponential behavior of attenuation, projection data contain signals from a ray through the entire body. Thus, this simplified rule of thumb actually yields more sampling than theoretically required. In our case, approximately 60 pixels spanned a planar image of the body, and recognizing it as a compromise, we chose to use 128 projections and not 180, because this was the maximum number of projections obtainable with the camera system available to us.

In order to preserve the spatial resolution in the digital projection data, we wanted to use a reconstruction filter with a relatively high cut-off frequency. We started with a ramp filter (i.e., that filter with the highest allowable cutoff and no smoothing), and worked "backward" with Butterworth filters with 1.4, 1.2, 1.0 and 0.8 cycles/cm cutoffs. We took 10 studies and reconstructed them with these filters and compared the anatomic detail to that in the corresponding CT images. The Butterworth filter with a 1.4 cycle/cm cutoff provided good anatomic detail, with the additional benefit of modest noise reduction (which the ramp filter could not provide) (Fig. 10). We thus standardized on this filter for all the data in this study.

Planar images were interpreted from hard-copy film, while SPECT images were directly viewed on the computer monitor (Fig. 11).

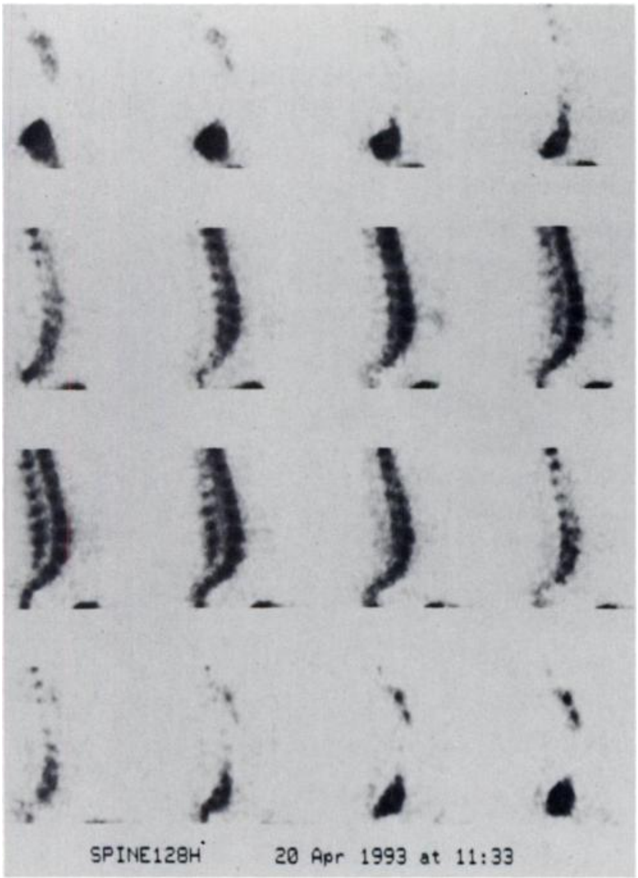

FIGURE 9. Sagittal slices reconstructed from transaxial slice data that were 2 pixels thick. Displayed from right, upper left to left, lower right.

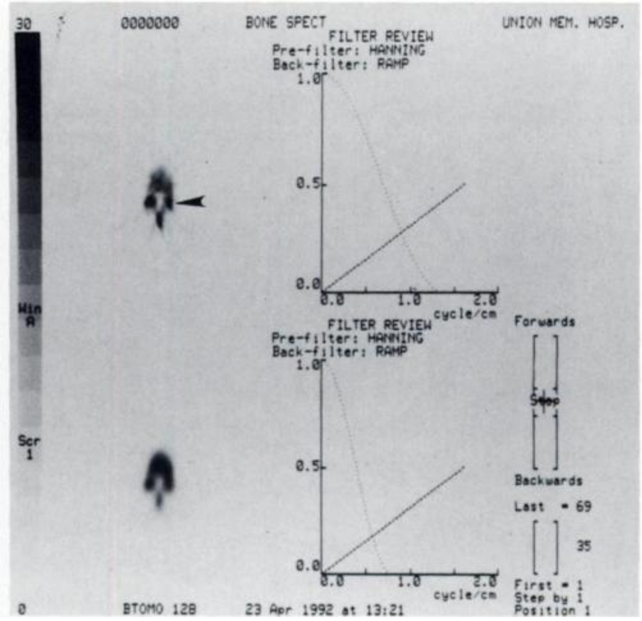

FIGURE 10. Effect of change in filter critical frequency. (Top) Critical frequency 1.4 retains both more data and more noise, yielding a mottled, but more accurate image. Note definition of the abnormal left facet joint (arrowhead), in addition to abnormal right side. (Bottom) Critical frequency 0.8 eliminates both noise and data resulting in a smoother, but less anatomically precise image. There is less certainty about the abnormal uptake at left facet joint.

Patient Classification

Facet joints identified as having abnormal increased tracer uptake were correlated with clinical symptoms, and when appropriate and severe enough to warrant an invasive procedure, facet injections with a marcaine and steroid mixture were subsequently performed with standard neuroradiology techniques under fluoroscopic guidance (*10*). Follow-up consisted of independent clinical evaluation of injection effectiveness, the review of a pain journal completed by the patient after injection, and long-term patient follow-up. Criteria for a final diagnosis of facet syndrome included initial clinical presentation, abnormal anatomic image, clinical follow-up including pain journal and outcome of treatment interventions, and a sustained positive response to facet injection, which was considered the most accurate indication of a facet etiology for pain.

RESULTS

Final clinical diagnoses and their relationship to radionuclide imaging are listed in Table 1. Nineteen patients demonstrated a total of 42 facet joints with abnormal increased tracer accumulation (Fig. 5B) and are detailed in Table 2. In nine of these patients, abnormal facet joint uptake correlated with clinical symptoms. Seven of these patients had a positive response to a facet injection, and were given a final diagnosis of facet syndrome. Two patients with strong clinical presentations, abnormal anatomic studies, positive response to treatment and clinical follow-up refused injection and were considered probable facet syndrome. They were not considered as either true-positive or false-positive for statistical analysis. Five other patients had facet injections. One patient with temporary pain relief was given a final diagnosis of spinal stenosis based on the total clinical evaluation including MRI. Four patients had no response to the injection. Their final diagnoses were lumbar spondylosis with degenerative joint dis-

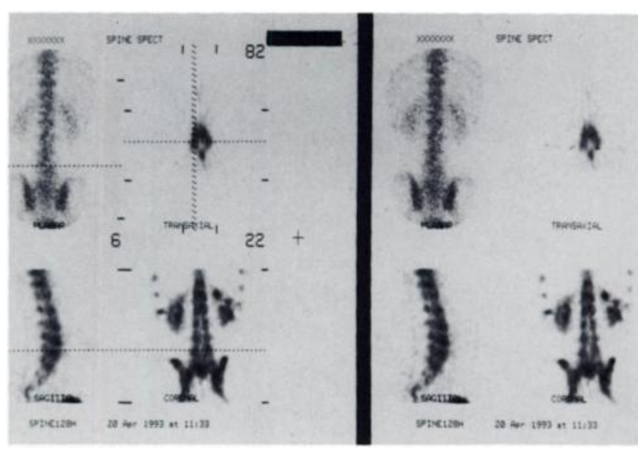

FIGURE 11. Normal SPECT. Computer viewing screen technique for multiplanar reconstructions. Localizing lines removed from right image. Reproductions illustrate difficulty of transferring digital data from screen to hard copy.

TABLE 1
Final Diagnosis and Relationship to Radionuclide Imaging

Diagnosis	Total patients*	Established by RNBI†
Facet syndrome	7‡	7
Probable facet syndrome	2§	2
Chronic lumbar DJD	11	8
Lumbar strain	5	0
Sacroiliac arthritis	4	1
Symptoms resolved	3	0
Spinal stenosis	2	0
Thoracic vertebrae compression fracture	2	1
Bladder problem	1	0
Facet arthrosis	1	1
Hip arthritis	1	1
Iliac fracture	1	1
Ischial tendinitis	1	0
Lumbar disk disease	1	0
Metastasis to L2 vertebra	1	1
Myofascial pain	1	0
Pars fracture	1	1
Rib fracture	1	1
Scheuermann's disease	1	0
Unexplained nerve root compression	1	0
Vascular disease in leg	1	0

*Six patients had more than one diagnosis. Chronic lumbar DJD and facet syndrome (2), chronic DJD and ischial tendinitis (1), chronic DJD and vascular disease (1), lumbar strain and thoracic compression fracture (1), rib fracture and SI arthritis (1).

†RNBI radionuclide bone imaging.

‡Two of seven patients had symptoms for 6 mo or less (3 and 6), two for 7 mo, three for 2 yr

§These two patients are not included in statistical analysis (Tables 3 and 4)

ease (n = 2), lumbar strain (n = 1) and facet arthrosis (focal arthritis) (n = 1). Five other patients with abnormal facet joint uptake, in addition to the two with facet syndrome who refused injection, were not injected for the following reasons: symptoms were not consistent with facet syndrome at follow-up (n = 2), symptoms were on the contralateral side to the abnormal facet uptake (n = 2), and symptoms improved on NSAID therapy (n = 1). Those 10 patients who had abnormal facet uptake, but who did not have facet syndrome or probable facet syndrome, included four with lumbar degenerative joint disease and one each with facet arthrosis, ischial tendinitis, lumbar strain, spinal stenosis, spontaneously rapidly resolved symptoms and vascular surgery and chronic degenerative joint disease.

The analysis of facet joint uptake by planar and SPECT techniques is detailed in Table 2 and analyzed in Table 3. SPECT imaging found abnormal facet uptake (n = 5) in four patients who had normal planar images (Fig. 12). Two of these patients were injected and both had a positive response to facet injection with a diagnosis of facet syndrome made. The other two patients were not injected; one had lumbar DJD and one lumbar DJD and vascular disease of the lower extremity.

Five other patients each had one additional facet with abnormal uptake on SPECT. Four of these patients had facet injections (all in conjunction with another abnormal facet also seen on planar images). One patient had a positive response and a diagnosis of facet syndrome, one had minimal temporary relief and had a final diagnosis of spinal stenosis, while two who had no response had a final diagnosis of chronic lumbar DJD. Therefore, a total of 10 facet joints with abnormal increased uptake were seen on SPECT which were not demonstrated on planar imaging.

SPECT imaging in addition better localized three out of 32 facet joints also seen on planar imaging. One of these was injected with good results and a final diagnosis of facet syndrome made. One of these was the patient with minimal temporary response to injection who had a final diagnosis of spinal stenosis, and one was not injected because his total clinical picture suggested DJD. There was no abnormal facet uptake seen on planar imaging which was not also seen on SPECT imaging. The relationships between the final clinical diagnosis and the scintigraphic findings and the resultant sensitivity, specificity and predictive values for the planar and SPECT techniques are listed in Tables 3 and 4.

TABLE 2
Analysis of Facet Joint Uptake by Planar and SPECT Techniques

	Patients				Lesions	
Scan findings	Planar normal	Planar abnor	SPECT normal	SPECT abnor	Planar	SPECT
Planar normal SPECT normal	24	0	24	0	0	0
Planar normal SPECT abnormal	4	0	0	4	0	5
Planar abnormal SPECT normal	0	0	0	0	0	0
Planar abnormal SPECT abnormal	0	15	0	15	32	37
Total						
Same number of lesions; no improvement with SPECT	0	9	0	9	24	24
Same number lesions, SPECT improved localization	0	1	0	1*	2	2
1–2 more lesions seen on SPECT, than on planar	0	5	0	5†	6	11

*In one patient, only one of two lesions seen had improved localization by SPECT.

†In two patients, SPECT both demonstrated additional abnormal uptake in one facet and improved localization in another, so that three total lesions seen in three different patients were better localized with SPECT.

TABLE 3
Final Clinical Diagnosis with Planar and SPECT Techniques*

	Facet syndrome	No facet syndrome
Planar diagnosis		
Facet abnormal	5	8
Facet normal	2	26
SPECT diagnosis		
Facet abnormal	7	10
Facet normal	0	24

*Based upon 41 patients, because the two patients with probable facet syndrome are not included in this data analysis as either true or false-positive studies.

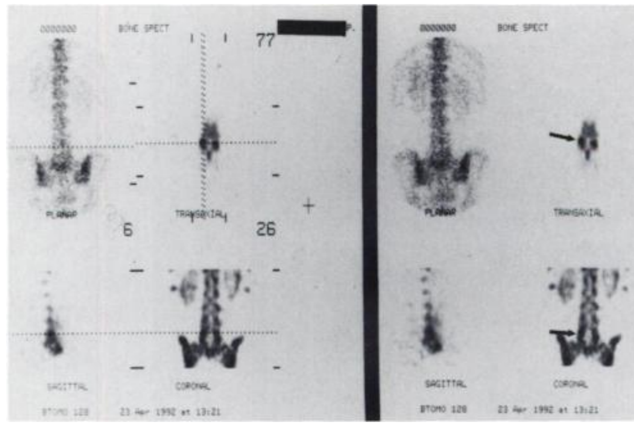

FIGURE 12. Facet syndrome. Normal planar, abnormal SPECT in a 51-yr-old female with a 3-mo history of pain. Bilateral abnormal uptake (arrows).

DISCUSSION

Improved preparation of cross-sectional cadaver specimens (*11*) (Fig. 1) has increased anatomic understanding, and cross-sectional imaging techniques (Figs. 3, 4) have supplemented plain radiographic imaging (Fig. 2) for diagnosis and have allowed for more precise anatomic analysis of the facet joints, but have not proved incrementally useful in identifying symptomatic lesions. Because low back and related pain is such a common problem, with significant economic consequences both to the afflicted individual and to society as a whole, any examination which has the potential to provide early diagnosis, and make more cost-effective use of expensive, invasive procedures deserves investigation. Despite advances in technology, the anatomic localization of abnormal pathophysiologic tracer uptake demonstrated on radionuclide bone imaging (Figs. 5 and 10, bottom) is often not accepted by the referring physician, in part we believe, because of their inability to confidently correlate the bone scan with the high-resolution radiographic, MR or CT images available to them. Speculation that less-smoothed SPECT images might both give more precise tracer localization and be accepted by the surgeons, coupled with the diagnostic dilemma of facet syndrome, led to the current study.

The development of the acquisition parameters for the SPECT technique reported in this paper was based upon theoretical considerations. We optimized the SPECT acquisition and processing protocol to maximize reconstructed image quality by maximizing the images' signal-to-noise ratio. In general, we considered the signal to be the contrast between bone and surrounding tissue, and the noise to be the statistical variation within bone. In the case of bone SPECT, the relatively high bone radiotracer uptake provided both high contrast and low noise. Thus, we designed a protocol which emphasized high spatial resolution, through collimator selection and projection sampling.

Final processing parameters were chosen empirically after production of multiple reconstructions, correlation with plain film and CT images and review with operating surgeons. As demonstrated in Figure 10, increasing the critical frequency of the Hanning pre-filter retains both more data and more noise with a mottled, but more accurate image.

Whenever a physiologic study is utilized, the clinical significance of observed changes must be assessed. Planar and SPECT bone imaging techniques often demonstrate small areas of minimal abnormal tracer accumulation, the significance of which is uncertain. That problem is greater with SPECT imaging because of the increased contrast enhancement inherent in that technique. This exquisite sensitivity to small increases in bone turnover is evidenced by the relatively low specificity of both SPECT (71%) and planar (76%) imaging in this study.

Since the facet injection procedure is considered by many to be simultaneously diagnostic and therapeutic, the real value of radionuclide imaging is to select appropriate patients for this invasive procedure. This is reflected in the high negative predictive value of SPECT (100%) and planar imaging (93%). The ability to identify other symptomatic abnormal areas of tracer uptake and characterize the underlying pathology (16 of 43 patients in this study) is an-

TABLE 4
Sensitivity, Specificity and Predictive Values for Planar Scintigraphy and SPECT

Patient (n = 41)	Planar	SPECT
Sensitivity $\frac{TP}{TP+FN}$	0.71	1.0
Specificity $\frac{TN}{TN+FP}$	0.76	0.71
Positive predictive value $\frac{TP}{TP+FP}$	0.38	0.41
Negative predictive value $\frac{TN}{TN+FN}$	0.93	1.0

other advantage of radionuclide bone imaging in patients who have unexplained pain of potentially osseous origin.

CONCLUSION

Both planar and SPECT radionuclide bone imaging are excellent modalities for evaluating low back pain potentially due to facet syndrome. The high negative predictive value of SPECT (100%) and planar images (93%) allow more efficacious selection of patients with symptoms suggesting facet syndrome who should receive diagnostic and therapeutic facet blocks. SPECT should be added to routine planar images if there is a need to better localize a focus of abnormal tracer uptake or if the patient's clinical symptoms strongly suggest facet syndrome and planar images are nondiagnostic. SPECT alone can be performed, but with most current cameras, less overall body area will be amenable to diagnosis and many minimal areas of uptake seen on SPECT images will have uncertain clinical significance.

Radionuclide bone imaging did discover other nonfacet lesions in 16 patients which were thought to be related to the patients' symptoms and therefore aided in establishing a final diagnosis (*12*). Eight of these had symptomatic chronic lumbar DJD, two of whom had superimposed facet syndrome at another level.

ACKNOWLEDGMENTS

The authors thank Charlie Barrett, PhD, who provided the anatomic section; Dr. Mike Rothman, for his suggestions; David Crandall, who produced the prints; Linda Clarke who typed the manuscript; Lisa Cole, BS, who helped with the initial SPECT acquisitions; Patty Sheehan, BS, and her nuclear medicine technology staff at the Union Memorial Hospital who obtained the clinical images; and Carol Smith and Ruth Taylor who aided with clinical follow-up. This material was first presented as a scientific exhibit at the 40th Annual Meeting at the Society of Nuclear Medicine, Toronto, Canada, June 1993. Financial support for the preparation of that exhibit was provided by the DuPont Company.

REFERENCES

1. Jackson RP. The facet syndrome: myth or reality. *Clinic Orthop* 1992;179: 110–121.
2. Bellah RD, Summerville DA, Treves ST, Micheli LJ. Low back pain in adolescent athletes: detection of stress injury to the pars interarticularis with SPECT. *Radiology* 1991;180:509–512.
3. Dussault RG, Lander PH. Imaging of the facet joints. *Radiol Clin North Am* 1990;27:1033–1053.
4. Ghormley RK. Low back pain with special reference to the articular facets with presentation of an operative procedure. *JAMA* 1933;101:10773–10777.
5. Mooney V, Robertson J. The facet syndrome. *Clin Orthop* 1976;115:149–156.
6. Berquist TH, ed. *Imaging of orthopedic trauma and surgery*. Philadelphia: W. B. Saunders Company; 1986:777–782.
7. Collier BD, Johnson RP, Carrera GF, et al. Painful spondylolysis or spondylolisthesis studied by radiography and single photon emission computed tomography. *Radiology* 1985;154:207–211.
8. Gates GF. SPECT imaging of the lumbosacral spine and pelvis. *Clin Nucl Med* 1988;13:907–914.
9. Ryan PJ, Evans PA, Gibson T, Fogelman I. Chronic low back pain: comparison of bone SPECT with radiography and CT. *Radiology* 1992;182:849–854.
10. Bogduk N. Back pain: zygapophyseal blocks and epidural steroids. In: Cousins MJ, Bridenbaugh PO, eds. *Neural blockade in clinical anesthesia and management of pain*, second edition. Philadelphia: J.B. Lippincott Co.; 1988:935–954.
11. Barrett CP, Anderson L, Holder LE, Poliakoff SJ. *Primer of sectional anatomy with MRI and CT correlation*, second edition. Baltimore: Williams & Wilkins; 1994.
12. Holder LE. Radionuclide bone imaging. *Radiology* 1990;179:607–614.